Probing the surface states in Bi_2Se_3 using the Shubnikov–de Haas effect

M. Petrushevsky,[1] E. Lahoud,[2] A. Ron,[1] E. Maniv,[1] I. Diamant,[1] I. Neder,[1] S. Wiedmann,[3] V. K. Guduru,[3] F. Chiappini,[3] U. Zeitler,[3] J. C. Maan,[3] K. Chashka,[2] A. Kanigel,[2] and Y. Dagan[1,*]

[1]*Raymond and Beverly Sackler School of Physics and Astronomy, Tel-Aviv University, Tel Aviv, 69978, Israel*

[2]*Department of Physics, Technion-Israel Institute of Technology, Haifa 32000, Israel*

[3]*High Field Magnet Laboratory, Institute for Molecules and Materials, Radboud University Nijmegen, Toernooiveld 7, NL-6525 ED Nijmegen, The Netherlands*

(Received 3 June 2011; revised manuscript received 22 February 2012; published 26 July 2012)

Shubnikov–de Haas oscillations are observed in Bi_2Se_3 flakes with high carrier concentration and low bulk mobility. These oscillations probe the protected surface states and enable us to extract their carrier concentration, effective mass, and Dingle temperature. The Fermi momentum obtained is in agreement with angle-resolved photoemission spectroscopy measurements performed on crystals from the same batch. We study the behavior of the Berry phase as a function of magnetic fields. The standard theoretical considerations fail to explain the observed behavior.

DOI: 10.1103/PhysRevB.86.045131 PACS number(s): 71.18.+y, 73.25.+i, 72.20.My, 79.60.−i

I. INTRODUCTION

The recently discovered topological insulators are a matter of intense theoretical and experimental study in contemporary condensed matter physics (for a review of the field, see Ref. 1). The exotic surface states that occur in these materials were confirmed and thoroughly studied using surface sensitive techniques, such as angle-resolved photoemission spectroscopy (ARPES)[2] and scanning tunneling microscopy (STM).[3] These measurements demonstrated the absence of backscattering at the surface, which is believed to be protected by time-reversal symmetry.

Of the three-dimensional (3D) topological insulators, Bi_2Se_3 has the simplest band structure—a single surface Dirac cone; however, transport experiments on this material present a challenge. The surface conducting state in Bi_2Se_3 is difficult to separate from the spurious bulk conductivity, believed to originate from Se vacancies.[4–6] Even in the lowest carrier-concentration samples metallic bulk behavior is observed. A few successful attempts to surmount this problem were reported, including thinning down the 3D material to decrease the bulk contribution,[7–10] using gate voltage,[11,12] pulsed high magnetic fields,[13] and changing the material composition to reduce the bulk conductivity.[5,14,15] However, providing conclusive transport evidence of the π Berry phase expected from the topology of the surface remains a challenge.

Recent attempts to probe the surface of Bi_2Se_3 crystals using the Shubnikov–de Haas (SdH) effect resulted in an overwhelming bulk signal.[6,16,17] These groups focused on making the samples cleaner in order to increase the bulk resistance. However, the decrease in the bulk carrier concentration led to an increased mobility. Consequently, the 3D oscillations dominated the signal.

In our work we adopt the opposite approach; the SdH effect has an exponential sensitivity on the mobility, whereas the conductance varies only linearly with it. This allows a mobility window in which the SdH effect probes only the protected surface states, albeit the dominance of the bulk over the classical conductance. This can be done by increasing the carrier concentration (thus lowering the bulk mobility), in contrast to the conventional approach.

Here we report on transport and ARPES measurements in Bi_2Se_3 flakes. We observe SdH oscillations in the magnetoresistance, and provide evidence that they originate solely from the surface Dirac cone. From these measurements we find the effective mass and carrier concentration and provide a lower bound for the Dingle scattering time. The ARPES data provides evidence of a single Dirac cone and the Fermi wave vector of the surface states obtained is in agreement with the magnetotransport result. We study the evolution of the SdH phase with magnetic fields. The broad field range studied and the pronounced oscillations observed result in unprecedented accuracy at which the frequency can be determined. However, we find that the phase is a strong function of the frequency. The data is consistent with a π Berry phase changing with magnetic field. However, the conventional Zeeman effect alone is insufficient to describe our data. Other possibilities, such as zero phase, are discussed.

II. METHODS

Single crystals of Bi_2Se_3 were grown in the standard method.[4,18] It is known that a Se-rich mixture usually results in a reduced carrier concentration in the bulk, as is the case in our reference sample with a carrier concentration of $\sim 10^{17}$ cm^{-3}. In order to get a rather high carrier concentration and low bulk mobility, we used a stoichiometric mixture of Bi (99.999%) and Se (99.99%), which was cooled down slowly at 3 °C/h and annealed for 24 h at 620 °C. This resulted in a carrier concentration of $\sim 10^{19}$ cm^{-3}. X-ray diffraction spectra (not shown) are consistent with previous reports of single crystals of Bi_2Se_3.[17]

Flakes $\sim 10-100$ μm thick were freshly cleaved perpendicular to the C_3 axis from a single crystal in a nitrogen environment (samples S1–S5). Gold contact wires were attached to the sample using silver paint. Measurements up to 14 T were performed in a Quantum Design PPMS platform using a Keithley 6221 current source coupled to a Keithley nanovoltmeter 2182 A. High field measurements (up to 33 T) were performed in the High Field Magnetic Laboratory with an SR830 DSP lock-in amplifier. For SdH

measurements flakes were cut into narrow bars and measured in a four-contact configuration. Other pieces from the same batch were measured in five-contact and Van der Pauw configurations for a more accurate determination of the resistivity and Hall coefficient. Two Hall probes were used for accurate determination of the perpendicular and parallel field components. ARPES measurements were performed using the He Iα line ($h\nu = 21.2$ eV) from a Scienta UV lamp and with an R4000 Scienta analyzer. The crystals for the ARPES measurement were cleaved *in situ* at vacuum better than 5×10^{-11} torr at 20 K.

We took extra care to properly align our voltage leads. Misaligned contacts resulted in a spurious Hall contribution in the longitudinal voltage channel. This contribution manifested itself in an antisymmetric background and a phase shift between positive and negative magnetic fields. Although all samples gave similar frequencies, samples with such Hall contribution were not used for the phase analysis.

III. RESULTS AND DISCUSSION

In the insets of Fig. 1 we show typical transport properties of a sample with high carrier concentration. The resistivity as a function of temperature for a typical flake is shown in the left inset. A metallic temperature dependence with a saturation value of $\sim 280\ \mu\Omega$ cm below 20 K is observed. The carrier concentration of this flake inferred from the Hall resistance at 2 K (see right inset) is 5.6×10^{19} cm^{-3}; this gives a bulk mobility of 400 cm^2/V s. Other samples in the literature have lower carrier density and higher mobilities.[6,16] These studies also show samples with higher carrier concentration $\sim 10^{19}$ cm^{-3}; however, their bulk mobility is at least a factor of 2 higher. Apparently, all these reported mobilities are high enough to obscure surface oscillations. Moreover, our reference (nonstoichiometric) samples with $n \sim 10^{17}$ cm^{-3} have similar properties as other samples in the literature[16] exhibiting 3D oscillations (see Appendix D).

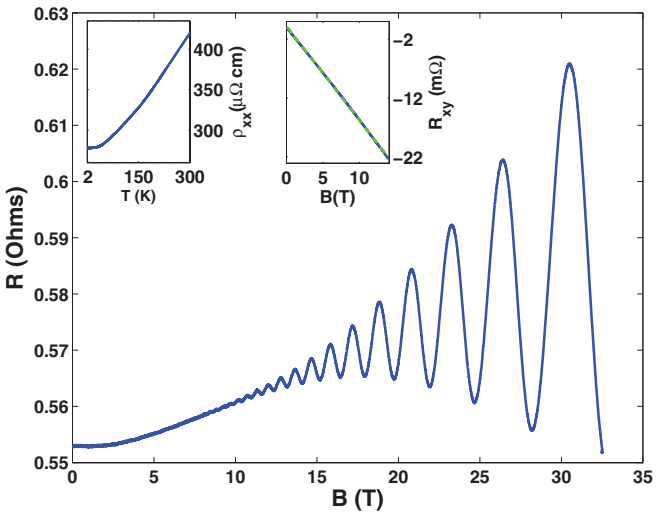

FIG. 1. (Color online) Resistance as a function of field for a high carrier concentration sample (S1) at $T = 4.2$ K in a perpendicular magnetic field up to 32.5 T. Left inset: typical longitudinal resistance versus temperature at $H = 0$. Right inset: Hall resistance as a function of magnetic field at $T = 2$ K, $H \parallel C_3$ axis. The dashed line is a linear fit yielding a charge carrier concentration of 5.6×10^{19} cm^{-3}. From the sign of the Hall slope we find that the charge carriers are electrons.

The resistance versus magnetic field at 4.2 K is shown in Fig. 1. Strong oscillations are observed. Below we analyze the oscillations and show evidence that they arise from the topological surface states.

According to the Onsager relation[19]

$$F = \frac{\hbar}{2\pi e} A(\epsilon_F), \tag{1}$$

the frequency of the SdH oscillations F is proportional to $A(\epsilon_F)$, the cross section of the Fermi surface in the plane perpendicular to the applied magnetic field. $\hbar$ is Planck's constant and e is the electron charge. For the case of a two-dimensional (2D) Fermi surface, $F \propto \frac{1}{\cos\theta}$, where θ is the angle between the normal to the 2D plane and the direction of the magnetic field. In Fig. 2 we show that our data follows the expected behavior of a 2D Fermi surface. Here θ is the angle between the C_3 axis and the applied magnetic field. For $\theta = 0$, we find frequencies in the range of 190−198 T for S1–S5.

The behavior shown in Fig. 2 is in strong contrast with measurements of our low carrier-concentration samples. For these flakes, $F = 20,26T$ for $H \parallel C_3$ and $H \perp C_3$, respectively. This corresponds to a 3D carrier density of 6.6×10^{17} cm^{-3},[20] consistent with Hall measurements (data are presented in Appendix D).

Substituting the average frequency $F = 195T$ in Eq. (1) and assuming a circular Fermi surface, we find $k_F = 0.077 \pm 0.003$ Å^{-1}, which corresponds to a 2D carrier density of $n_{2D} = \frac{k_F^2}{4\pi} = 4.7 \times 10^{12}$ cm^{-2}, assuming no spin degeneracy, as should be the case for a topologically protected surface.

Figure 3 presents ARPES data from a cut taken along the ΓM direction and going through the Γ point on a typical

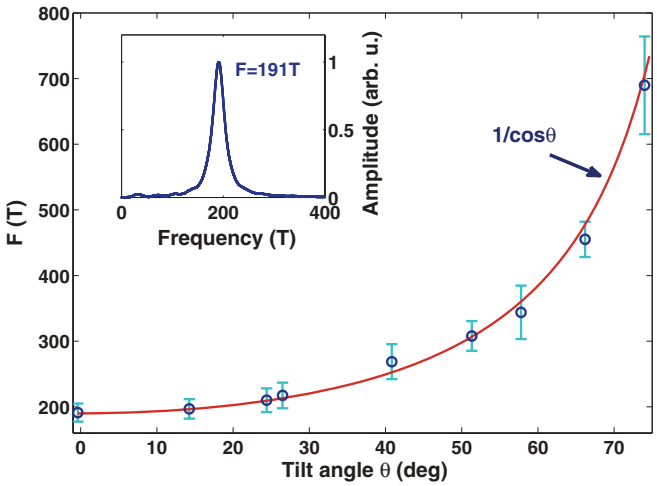

FIG. 2. (Color online) Frequency of the oscillations measured in S2 as a function of θ (all other samples from this batch exhibited similar behavior). The bars represent the full width at half maximum of the FFTs, which are an upper bound for the error. The solid line is the expected 2D $\frac{1}{\cos\theta}$ behavior.

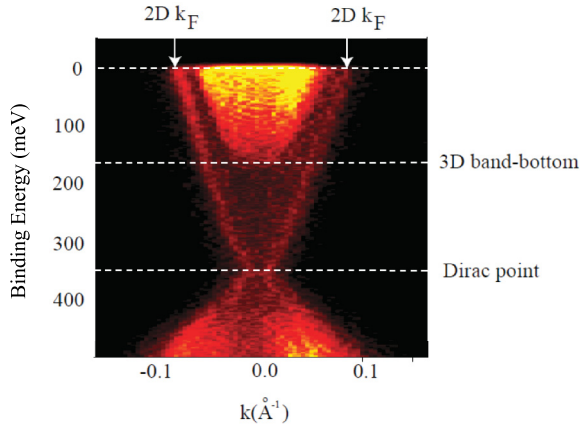

FIG. 3. (Color online) ARPES band dispersion of a high carrier concentration sample. Both the bulk and the surface states are observed in the data. The dashed lines mark the bottom of the 3D band (around 160 meV below the Fermi level) and the Dirac point (around 345 meV below the Fermi level). The arrows mark k_F of the 2D surface state ($k_F = 0.084 \pm 0.005$ Å^{-1}).

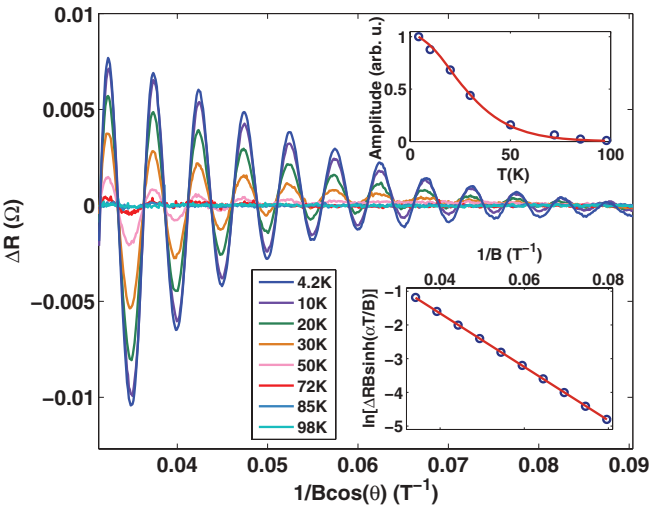

FIG. 4. (Color online) Temperature dependence of the SdH oscillations at $\theta = 0$ after subtracting a smooth polynomial background (S3). Top inset shows the temperature dependence of the amplitude, yielding $m^* \simeq 0.16 m_e$. Bottom inset: a Dingle plot resulting in $\tau_D = (3.6 \pm 0.4) \times 10^{-14}$ s.

flake. The contribution of the bulk electrons as well as the Dirac-like surface state are clearly seen. We find $k_F = 0.084 \pm 0.005$ Å^{-1} in agreement with the value extracted from the SdH analysis.

The resistance of a 2D system exhibiting SdH oscillations is given by[19]

$$R_s{}^{2D} = R_0 \left\{ 1 + R_T R_D \cos\left[2\pi \left(\frac{F}{B} + \frac{1}{2} + \beta \right) \right] \right\}, \quad (2)$$

where R_0 is the zero field resistance and $2\pi\beta$ is the Berry phase which is expected to be π for an electron rotating around the Dirac point in a topological insulator at the low magnetic field limit.[1] R_T contains the temperature dependence,

$$R_T = \frac{\alpha T}{B} \Big/ \sinh\left(\frac{\alpha T}{B} \right) \quad (3)$$

with $\alpha = \frac{2\pi^2 m^* k_B}{\hbar e}$. The dingle factor is

$$R_D = \exp\left(\frac{-\pi}{\omega_c \tau_D} \right), \quad (4)$$

where τ_D is the dingle scattering time, and corresponds to the dephasing of the Landau states. $\omega_c = \frac{eB}{m^*}$ is the cyclotron frequency. R_D determines the amplitude decay with the decrease of magnetic field.

The standard analysis of SdH oscillations yields a cyclotron mass of $m^* \simeq 0.16 m_e$ (Ref. 23; see Fig. 4); this together with the field dependence of the oscillation amplitude at 4.2 K gives $\tau_D = (3.6 \pm 0.4) \times 10^{-14}$ s, a Dingle temperature of $T_D = \frac{\hbar}{2\pi\tau_D k_B} = 33.78 \pm 0.33$ K, and a corresponding quantum mobility of $\mu_q^{2D} = 400$ cm^2/V s.

Further confirmation of the 2D nature of the oscillations reported here is inferred from a comparison between the quantum (Dingle) and transport mobilities. Forcing a 3D fit to the amplitude of the oscillations (which contains an additional $\sqrt{B}$ coefficient), one finds a 3D Dingle time of 3.9×10^{-14} s which corresponds to a bulk quantum mobility of $\mu_q^{3D} = 570$ cm^2/V s, larger than the transport mobility $\mu_{tr}^{3D} = 400$ cm^2/V s. This is in strong contrast with recent reports for Bi_2Se_3, where the Dingle mobility is four times smaller than the transport one.[17] Furthermore, it is physically impossible to have $\mu_q^{3D} > \mu_{tr}^{3D}$ in a bulk material, since the Dingle mobility takes into account all scattering events, including small angle scattering, that usually do not affect the resistivity, whereas for the transport mobility, backscattering events play the major role.

One of the hallmarks of a topological insulator is the π Berry phase associated with the Dirac dispersion relation. Since pronounced oscillations are observed in a broad field range (see Fig. 1), we are able to follow the evolution of the Berry phase as a function of applied magnetic field for S1.

The standard phase analysis is done by plotting F/B versus n, the oscillation index (usually referred to as the Landau-level fan diagram). Applying this to our data, using the FFT peak $F = 198$ T yields a zero phase ($\beta = 0$). We note that due to the many oscillations measured, the Fourier transform analysis favors a frequency that yields a zero phase. Furthermore, we find that β is very sensitive to F, and even a deviation of 1.5%, which is well within the error margin, has a strong effect on β. For example, if we take $F = 195$ T, we get a π Berry phase ($\beta = 0.5$) at low fields, deviating towards zero as the field increases. In the following, we study the behavior of β for frequencies in the vicinity of the FFT peak, $F = 198 \pm 3$ T.

In order to focus on the field and frequency dependencies of the phase, we use the relation

$$\beta(F,n) = n - F/B \quad (5)$$

and plot β versus n in Fig. 5, where n is the index of the oscillation minima for the two frequencies mentioned (see Appendixes A and B for more details and an analysis on more samples). The two behaviors mentioned above are now clearly seen. This analysis casts strong doubts on the

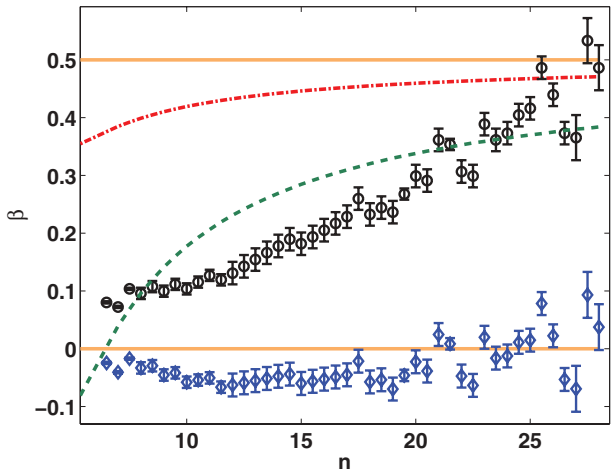

FIG. 5. (Color online) Analysis of the Berry phase $2\pi\beta$ according to Eq. (5) using the data from Fig. 1 after subtracting a smooth polynomial background. $n = 6.5$ corresponds to $B = 30.4$ T and $n = 28$ to $B = 7$ T. The blue diamonds are obtained using the FFT peak of $F = 198$ T, consistent with a zero Berry phase. The black circles correspond to $F = 195$ T, for which a π Berry phase is observed at low fields. This phase changes towards zero as the field increases. This demonstrates the strong sensitivity of the phase to the frequency chosen. The error bars stem from the freedom in choosing the oscillation extrema. The green dashed (red dashed-dotted) line is the expected behavior of β taking into account a Zeeman term with $g = 50$ (100), respectively.

ability to independently determine the Berry phase using SdH oscillations.

Assuming that at low field β should be 0.5, the simplest explanation for the phase change would be a Zeeman term in the Hamiltonian.[13] In Fig. 5 we plot the expected behavior of β using gyromagnetic ratios $g = 50, 100$ and $v_F = 6.24 \times 10^5$ m/s as inferred from the ARPES measurement (see Fig. 3). While both the theoretical curve ($g = 100$) and the measured data are in qualitative agreement, it is obvious that this simple model is insufficient to describe our measurements. It is possible that the nonideality of the Dirac dispersion should also be taken into account.[21]

IV. CONCLUSION

In summary, we present evidence that the surface states in Bi_2Se_3 can be probed in highly conducting flakes using the SdH effect. This is in contrast with the conventional approach focused on improving the crystal purity. From the SdH analysis we find for the surface states $m^* = 0.16m_e$, $\tau_D = (3.6 \pm 0.4) \times 10^{-14}$ s. The Fermi momentum is in agreement with the ARPES data obtained on a flake from the same batch. We carefully study the behavior of the Berry phase with magnetic field, and show that two scenarios are possible: $\beta = 0.5$ (π Berry phase) at low magnetic fields which changes fairly quickly with magnetic field, or a trivial zero phase. Two major issues are yet to be understood: first, the survival of protected surface states despite the large bulk conductivity, and second, the peculiar behavior of the Berry phase with magnetic field.

ACKNOWLEDGMENTS

The work at Tel Aviv University is supported by the Israel Science Foundation (ISF) under Grant No. 1421/08 and the Ministry of Science and Technology. Part of this work has been supported by EuroMagNET under the EU Contract No. 228043.

APPENDIX A : ZEEMAN EFFECT ON $\beta(n)$

We use a simplified model of noninteracting electrons on the surface of topological insulators in a perpendicular external magnetic field. These electrons occupy orbital Landau levels which are coupled to their spin. The spin is also Zeeman coupled to the magnetic field. The energy of an electron in the nth orbital Landau level is therefore composed from both the orbital energy and the Zeeman energy in the following way (see, for example, Ref. 21):

$$E_n = \sqrt{\frac{1}{4}(g\mu_B B)^2 + 2n\hbar^2\left(\frac{v_F}{l_b}\right)^2}, \tag{A1}$$

where g is the effective gyromagnetic ratio for electrons on the surface, μ_B is the Bohr magneton, B is the magnetic field, v_F is the Fermi velocity associated with the Dirac cone, and $l_b = \sqrt{\frac{\hbar}{eB}}$ is the magnetic length. The nth maximum of the SdH oscillation in R_{xx} occurs at magnetic field $B_{n,\max}$ where this energy crosses the Fermi energy, $E_n = E_F$. This requirement and Eq. (A1) lead to

$$G B_{n,\max} + n = \frac{F_0}{B_{n,\max}}, \tag{A2}$$

where $G = \frac{1}{8e\hbar}(\frac{g^*\mu_B}{v_F})^2$ and $F_0 = E_F^2/2\hbar e v_F^2$. One can write a similar expression for the minimum of the oscillations which occurs halfway between the n and $n+1$ maxima. Interpolation of Eq. (A2) gives approximately (for large enough values

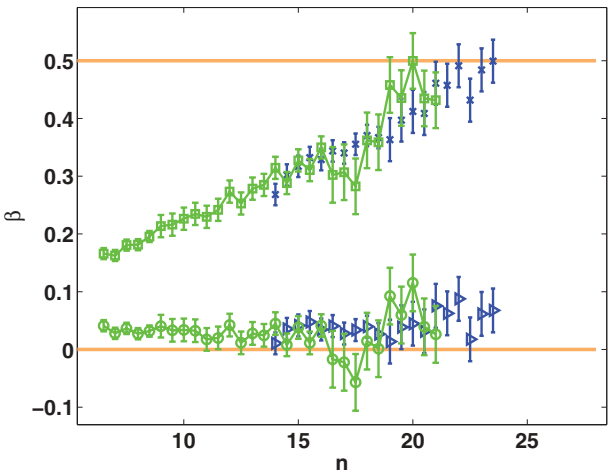

FIG. 6. (Color online) The behavior of $\beta(n)$ for S4 (green circles—196 T and squares—192.8 T) and S5 (blue ×'s—186.5 T and triangles—190 T).

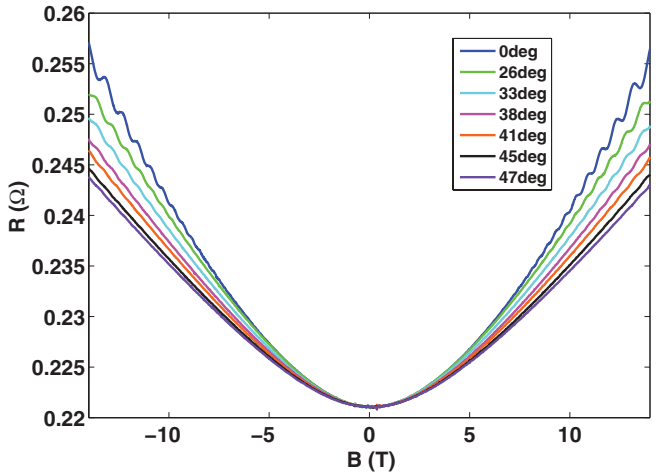

FIG. 7. (Color online) Resistance as a function of magnetic field for various tilt angles θ (S5).

of n),

$$GB_{n,\min} + n + \frac{1}{2} \simeq \frac{F_0}{B_{n,\min}}.$$

The phase of the oscillations is defined as in Eq. (5),

$$\beta(F,n) = n + \frac{1}{2} - \frac{F}{B_{n,\max}} \simeq n - \frac{F}{B_{n,\min}}. \qquad \text{(A3)}$$

In usual metals, this definition gives $\beta = 0$, independent of n, for the right choice of F. However, in our case, given the theoretical relation between n and $B_{n,\max(\min)}$ in Eqs. (A2) and (A3), β depends on n for any choice of F. We can choose $F = F_0$, which is the frequency of the oscillations in the limit of low magnetic fields, and we get for $n \gg 1$,

$$\beta(F_0,n) = 0.5 + GB_{n,\max} \simeq GB_{n,\min}.$$

APPENDIX B : FREQUENCY DEPENDENCE OF $\beta(n)$ FOR ADDITIONAL SAMPLES

In Fig. 6 we show the frequency dependence of $\beta(n)$ for additional samples—S4 and S5 (measured up to 33 and 14 T, respectively). One can see that this is similar to the behavior of S1 depicted in Fig. 5.

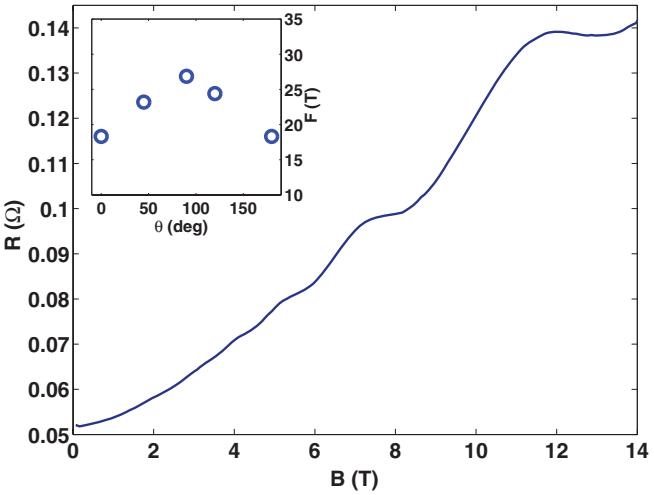

FIG. 8. (Color online) Typical oscillations in our lower carrier-concentration samples of $n \sim 10^{17}$ cm^{-3}. The inset is the typical 3D angular dependence of the oscillation frequency.

APPENDIX C : BULK MAGNETORESISTANCE

One may conjecture that the apparent 2D angular behavior is a result of some anomalous scattering occurring in the bulk when applying a parallel magnetic field component. To refute this claim we show in Fig. 7 the angular dependence of the magnetoresistance. One can see that the magnetoresistance decreases with θ. This implies that the bulk scattering time increases with tilt angle. Furthermore, the magnetoresistance as a function of perpendicular magnetic field is not constant, but slightly increasing. Thus a quasi-2D bulk is not likely as well.

APPENDIX D : LOWER CARRIER-CONCENTRATION SAMPLES

In Fig. 8 we demonstrate the typical 3D behavior observed in our reference, lower carrier-concentration samples with $n \sim 10^{17}$ cm^{-3}. These samples were prepared with a Se concentration higher than the stoichiometric one. This is done in order to reduce the number of Se vacancies and consequently the bulk conductance, resulting in increased mobility. The observed behavior for these samples is consistent with Ref. 16.

*yodagan@post.tau.ac.il

[1] M. Z. Hasan and C. L. Kane, Rev. Mod. Phys. **82**, 3045 (2010).
[2] Y. Xia, D. Qian, D. Hsieh, L. Wray, A. Pal, H. Lin, A. Bansil, D. Grauer, Y. S. Hor, R. J. Cava, and M. Z. Hasan, Nat. Phys. **5**, 398 (2009).
[3] P. Roushan, J. Seo, C. V. Parker, Y. S. Hor, D. Hsieh, D. Qian, A. Richardella, M. Z. Hasan, R. J. Cava, and A. Yazdani, Nature (London) **460**, 1106 (2005).
[4] G. Hyde, H. Beale, I. Spain, and J. Woollam, J. Phys. Chem. Solids **35**, 1719 (1974).
[5] J. G. Checkelsky, Y. S. Hor, M.-H. Liu, D.-X. Qu, R. J. Cava, and N. P. Ong, Phys. Rev. Lett. **103**, 246601 (2009).
[6] J. G. Analytis, J.-H. Chu, Y. Chen, F. Corredor, R. D. McDonald, Z. X. Shen, and I. R. Fisher, Phys. Rev. B **81**, 205407 (2010).
[7] H. Peng, K. Lai, D. Kong, S. Meister, Y. Chen, X.-L. Qi, S.-C. Zhang, Z.-X. Shen, and Y. Cui, Nature Mater. **9**, 225 (2010).
[8] H. Tang, D. Liang, R. L. J. Qiu, and X. P. A. Gao, ACS Nano **5**, 7510 (2011).
[9] Y. Zhang, K. He, C.-Z. Chang, C.-L. Song, L.-L. Wang, X. Chen, J.-F. Jia, Z. Fang, X. Dai, W.-Y. Shan, S.-Q. Shen, Q. Niu, X.-L. Qi, S.-C. Zhang, X.-C. Ma, and Q.-K. Xue, Nat. Phys. **6**, 584 (2010).
[10] Y. S. Kim, M. Brahlek, N. Bansal, E. Edrey, G. A. Kapilevich, K. Iida, M. Tanimura, Y. Horibe, S.-W. Cheong, and S. Oh, Phys. Rev. B **84**, 073109 (2011).

[11] J. Chen, H. J. Qin, F. Yang, J. Liu, T. Guan, F. M. Qu, G. H. Zhang, J. R. Shi, X. C. Xie, C. L. Yang, K. H. Wu, Y. Q. Li, and L. Lu, Phys. Rev. Lett. **105**, 176602 (2010).

[12] J. G. Checkelsky, Y. S. Hor, R. J. Cava, and N. P. Ong, Phys. Rev. Lett. **106**, 196801 (2011).

[13] J. G. Analytis, R. D. McDonald, S. C. Riggs, J.-H. Chu, G. S. Boebinger, and I. R. Fisher, Nat. Phys. **6**, 960 (2010).

[14] D. Hsieh, Y. Xia, D. Qian, L. Wray, J. H. Dil, F. Meier, J. Osterwalder, L. Patthey, J. G. Checkelsky, N. P. Ong, A. V. Fedorov, H. Lin, A. Bansil, D. Grauer, Y. S. Hor, R. J. Cava, and M. Z. Hasan, Nature (London) **460**, 1101 (2009).

[15] Z. Ren, A. A. Taskin, S. Sasaki, K. Segawa, and Y. Ando, Phys. Rev. B **82**, 241306 (2010).

[16] N. P. Butch, K. Kirshenbaum, P. Syers, A. B. Sushkov, G. S. Jenkins, H. D. Drew, and J. Paglione, Phys. Rev. B **81**, 241301 (2010).

[17] K. Eto, Z. Ren, A. A. Taskin, K. Segawa, and Y. Ando, Phys. Rev. B **81**, 195309 (2010).

[18] Y. Hor, J. Checkelsky, D. Qu, N. Ong, and R. Cava, J. Phys. Chem. Solids **72**, 572 (2011).

[19] D. Shoenberg, *Magnetic Oscillations in Metals* (Cambridge University Press, Cambridge, 1984).

[20] V. A. Kulbachinskii, N. Miura, H. Nakagawa, H. Arimoto, T. Ikaida, P. Lostak, and C. Drasar, Phys. Rev. B **59**, 15733 (1999).

[21] A. A. Taskin and Y. Ando, Phys. Rev. B **84**, 035301 (2011).

[22] K. S. Novoselov, A. K. Geim, S. V. Morozov, D. Jiang, M. I. Katsnelson, I. V. Grigorieva, S. V. Dubonos, and A. A. Firsov, Nature (London) **438**, 197 (2005).

[23] The cyclotron mass should not be zero even for the case of a linear dispersion relation. It is determined from the relation $m^* = E_F/v_F^2$ (Ref. 22).